16th IMEKO TC10 Conference
"Testing, Diagnostics & Inspection as a comprehensive value chain for Quality & Safety
Berlin, Germany, on September 3-4, 2019

Experimental Investigation of Single Point Incremental Forming of Aluminium Alloy Foils

Imre Paniti[1], Zsolt János Viharos[2], Dóra Harangozó[3]

[1]*Centre of Excellence in Production Informatics and Control, Institute for Computer Science and Control of the Hungarian Academy of Sciences, H-1111 Budapest, Kende u. 13-17., Hungary, imre.paniti@sztaki.mta.hu*
[2]*Centre of Excellence in Production Informatics and Control, Institute for Computer Science and Control of the Hungarian Academy of Sciences, H-1111 Budapest, Kende u. 13-17., Hungary, viharos.zsolt@sztaki.mta.hu*
[3]*Széchenyi István University, H-9026 Győr, Egyetem tér 1., Hungary, harangozo.dora@sze.hu*

***Abstract* – Incremental Sheet Forming is a prosperous process to manufacture sheet metal parts that is well adapted for prototypes or small batch production. Compared to traditional sheet forming technologies this relatively slow process is only profitable for the above mentioned production types but it can be used in different applications in automotive and aircraft industries, in architecture engineering and in medical aids manufacturing. In this paper indirectly obtained axial forming force on Single Point Incremental Forming (SPIF) of variable wall angle geometry were studied under different process parameters. The estimation of the forces on AlMn1Mg1 sheets with 0.22 mm initial thickness is performed by continuous monitoring of servo motor currents. The deformation states of the formed parts were analysed using the ARGUS optical strain measurement system of GOM. Interaction plot of forming speed, incremental depth, tool diameter and lubrication were also reported.**

Keywords – Incremental Sheet Forming, Rapid Prototyping, Optical Strain Measurement, Design of Experiments.

I. INTRODUCTION

Incremental Sheet Forming with its main groups (Single Point Incremental Forming – SPIF – and Two Point Incremental Forming – TPIF) is still an interesting research topic in Material Science because of its extreme and complex mode for deformation, the flexibility of the process and the high forming limits compared to traditional forming processes. Several articles are dealing with experimental study on force measurements for SPIF like [1] or [2], but only a couple of them are focusing on sheets with initial thickness less than 0.5mm [3-6].
Furthermore, as Gatea et al. [7] highlighted regarding the Fracture Forming Limit Curve (FFLC) in a review, that further investigation should be carried out into the effect of initial sheet thickness to tool radius ratio (t_0/R) on the FFLC, and whether it is enough to describe FFLC in SPIF. The above mentioned facts initialized this study to conduct experiments on AlMn1Mg1 sheets with 0.22 mm initial thickness. Former results of this research with the same material explained what kind of control system have been used to execute the tool path on this part [11], and how flat end tools can improve e.g. the accuracy of the part [12], so, the aim of this research work is twofold. At first, the goal is to apply a non-traditional force monitoring on AlMn1Mg1 foils and secondly, to experimentally validate main process parameters on sheets thinner than 0.5mm. The first part of this paper focuses on the material characterization introducing a Forming Limit Curve measured by Nakazima test; the second part of this paper presents preliminary investigations on the formability of truncated conical shapes with a continuously increasing wall angle as a function of major operating parameters. In addition, forming forces have been investigated experimentally with servomotor acquisitions.

II. DESCRIPTION OF THE METHOD

Single Point Incremental Forming experiments were carried out on a Rieckhoff CNC milling machine. The forming tool and a fast-clamping system is shown in Fig. 1(a). The number of experiments required to determine the forming limit of a sheet can be reduced by using a part geometry with variable wall angle as claimed in [8]. For this reason, a conical frustum with circular generatrix (model generating curve) design was used as shown in Fig. 1(b).
The CNC Machine control was realised with an open-source Real-Time Control Software called LinuxCNC. This control allowed to send the tool coordinates to a data acquisition program which collected also the Servomotor Current data of the Z-axis.

(a)

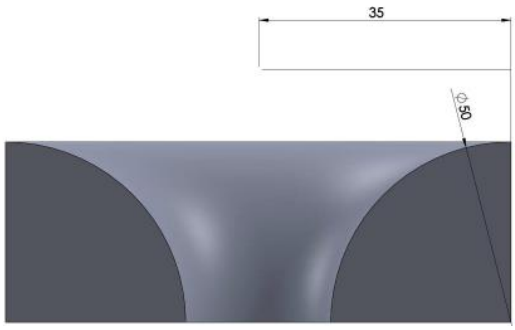

(b)

Fig. 1. (a) Set-up of the experiments, (b) Section view of the test geometry

The chemical composition of AlMn1Mg1 used for this study is given in Table 1. The tensile tests were carried out according to EN ISO 6892-1:2010 standard at room temperature using INSTRON 5582 universal testing machine. Specimens were cut from sheet in 0°, 45° and 90° to rolling direction. The planar anisotropy values (r) were evaluated from longitudinal and transversal strains measured by AVE video extensometer.

The mechanical properties are listed in Table 2. Result of Erichsen Cuping Test is IE=6.79 and Limiting Draw Ratio obtained from Cup Drawing Test according to Swift is LDR=1.7.

Table 1. Chemical composition of the sheet material.

Al	**Si**	**Fe**	**Cu**	**Mn**
96.90	0.201	0.448	0.212	0.807
Mg	**Zn**	**Cr**	**Ni**	**Others**
1.260	0.071	0.022	0.006	0.073

Table 2. Results of tensile tests.

Direction	**Rp0.2, MPa**	**Rm, MPa**	**Ag, %**
0°	88.3	183.0	16.44
45°	90.0	155.5	9.27
90°	86.3	170.3	12.48
A50, %	**n5**	**r10**	
16.88	0.297	0.554	
10.45	0.266	0.580	
12.98	0.268	0.594	

Fig. 2. illustrates the Forming Limit Curve (FLC) and Fracture Forming Limit Curve (FFLC) of tested sheet which were constructed from results of Nakazima test using a hemispherical tool of 50 mm in diameter and GOM ARAMIS digital optical measuring system. FLC curve was evaluated according to EN_ISO_12004-2-2009 standard. It is well known from the literature, that SPIF can achieve more times higher strains than it can achieve during conventional forming process like deep drawing. Therefore, forming limit in SPIF should be represented by Fracture Forming Limit Curve. Fracture limit strains of tested sheet were determined also from Nakazima test using ε_2-ε_1 plots of GOM evaluation system.

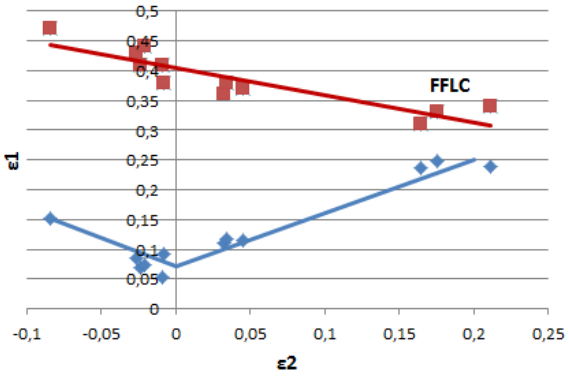

Fig 2. Forming and Fracture Forming Limit Curve

It should be noted that this FFLC seems not realistic as limit of Incremental Sheet Forming for many reasons. The main argue is that during Nakazima test local stretching deformation causes positive stress triaxiality factor while at SPIF the tool generates compressive stress in the sheet metal which might influence the stress triaxiality in negative direction and therefore higher strain limits can achieve. This effect is stronger at Double Point Incremental Forming where compressive load caused by tools is more significant. To realise this enhanced process two Parallel Kinematic Machines (PKMs) [13] or two Industrial Robots should be used [14]. In both cases the synchronisation of the two tools have to be solved. However, the same results can be achieved with one industrial robot, a C-frame, a linear actuator and a mechanical copying device [15].

More realistic values for limit strains can be found in literature. At plane strain (ε_2=0) the limit strain (ε_1=FLD_0) reaches 2.3 for AA1050-O (Filice et al., [16]) and 0.84 for AA6114-T4 while 3.0 for AA3003-O (Micari, [17]). These values show that significant scatter is among empirical values.

Applying the classical equation $t_f=t_0 \cdot \sin(90-\phi)$ (where t_f and t_0 are final and initial thicknesses, ϕ is wall angle) it can be calculated that if $\phi=60^o$ then logarithmic thickness reduction strain (FLD_0) is 0.9 and if $\phi=70^o$ then FLD_0=1.08. Initial wall thickness influences the limit strain, for example Kim et al. [18] showed that if thickness decreases from 0.5 mm to 0.3 mm the limit strain also decreases by 23% to FLD_0=0.92.

Jeswiet et al. [19] elaborated empirical formulae for

calculation of maximum wall angle for truncated conical specimens. The (1a) and (1b) equations show the influence of sheet thickness on wall angle as function of material.

$$\phi_{max}=8.5\ t_0 + 60.7 \quad \text{for AA3003-O} \quad (1a)$$
$$\phi_{max}=3.3\ t_0 + 58.3 \quad \text{for AA5754-O} \quad (1b)$$

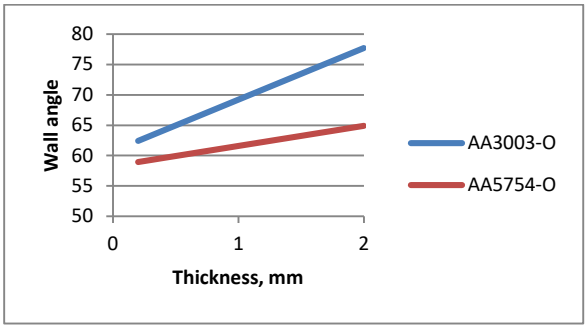

Fig. 3. Wall angle vs. sheet thickness

Fig. 3. shows that lower alloy content of AA3003 enables higher wall angle limits than AA5754 with 3.5% Mg content. At the same time, it is also visible that as the sheet thickness decreases the formability is also decreasing.

Empirical evaluation of local deformations was measured by GOM ARGUS system [20]. This technique uses a regular mesh on the surface of blank material (Fig. 4(b)). After forming process, the local deformations are calculated using ARGUS software. The results from the ARGUS system provide full-field information about major-minor strain, thickness reduction and geometric parameters of the sheet metal part.

III. RESULTS AND DISCUSSIONS

Table 3 shows the process parameters (F: forming speed, △Z: incremental depth, d: tool diameter) applied in the Design of Experiments (DOE, using L9 orthogonal array of Taguchi) and the examined output parameter, the Z coordinate where fraction occurred on the formed part (-Z frac.).

Table 3. Process parameters and results.

Exec. order	F (mm/min)	△Z(mm)	d (mm)	Lubricant	-Z frac. (mm)
1.	500	0.1	2.381	#3	22.32
5.	500	0.3	4	#2	20.16
9.	500	0.5	6	#1	19.60
4.	1750	0.1	4	#1	19.81
8.	1750	0.3	6	#3	19.93
3.	1750	0.5	2.381	#2	20.01
7.	3000	0.1	6	#2	18.95
2.	3000	0.3	2.381	#1	20.01
6.	3000	0.5	4	#3	20.10
1.	500	0.1	2.381	#3	22.32

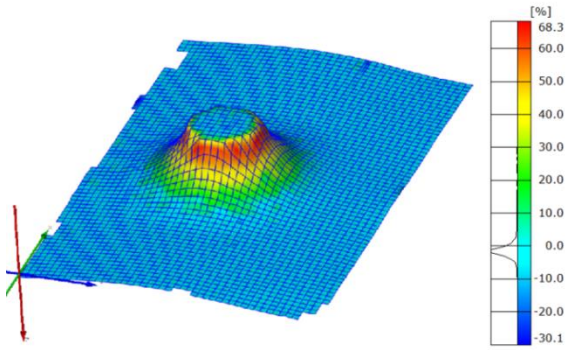

(a)

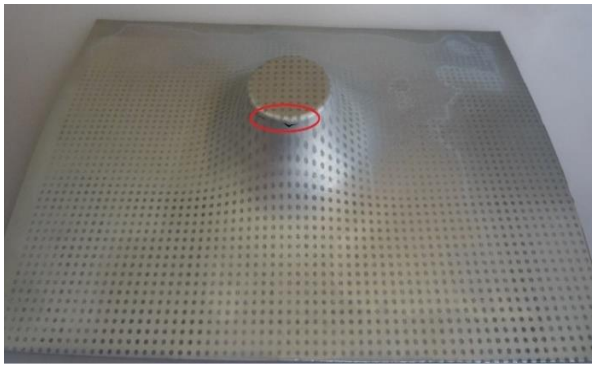

(b)

Fig. 4. (a) Thickness reduction of the first part, (b) Picture of the first formed part, indicating the fracture

Z axis loads were obtained to monitor the necking and fracture as in [9]. Fig. 4(a) shows the thickness reduction of the first formed part (from the GOM ARGUS system), while Fig. 4(b) shows a picture of the first formed with a fracture caused by necking.

By using the data of the motor and the drive train, the force applied by the axle as a function (2) of the motor current is the following:

$$F_{Z-current} = \frac{2\pi}{h} \cdot i_s \cdot \left(k_M \cdot I - M_R\right) \quad (2)$$

where:

- $F_{Z\text{-}current}$ – axial force applied by the ball screw nut [N]
- h – ball screw pitch [mm]
- i_s – transmission ratio of the belt drive
- k_M – motor constant [mNm/A]
- I – motor current [A]
- M_R – torque loss due to friction in the motor [mNm]

Similar methodology was used by Rauch et al. [10] to evaluate tool loads in a Parallel Kinematic Machine.

Fig. 5 shows the validation of the measurement concept, by comparing measurement results from a Force

Cell (Fz) with the calculated forces (Fz-current) from the motor current measurements.

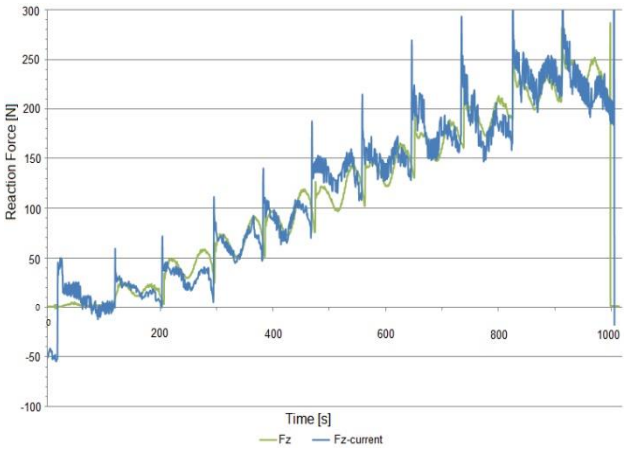

Fig. 5. Validation of the measurement concept

Current measurements were realised with a 0.33 Ohm electrical measurement resistance. From Ohms law the voltages on the CNC's Z axis can be obtained. The peaks in Fz-current are indicating the Z-level changes, where the tool pushes the sheet to reach the next depth level up to the fracture. Fz values are pre-filtered in quasi real-time to get a smoother value change. The reaction force (and the current) increases in the first phase of the forming as the sheet becomes harder to form. Fig. 6 shows the results of the first forming, indicating the values of the fracture (oval mark). In case local necking or fracture occurs, the voltage increases up around the starting value.

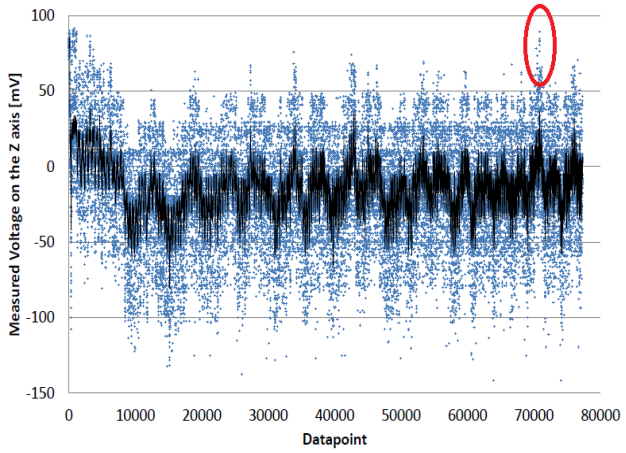

Fig. 6. Measured voltage on the Z axis by executing the forming of the first part and indicating the values of the fracture [11]

The major strain distribution in a dedicated section of the same part can be seen in Fig. 7. Major strain increased up to 126% (1.26) in the area of the fracture. Similar phenomena occur with thicker sheets.

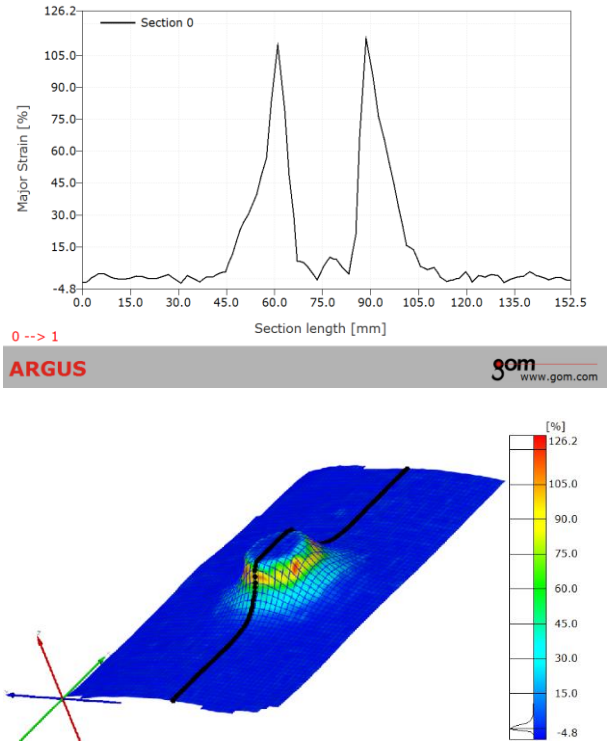

Fig. 7. Major strain distribution of the first part in a section

This value is similar to that of cited from the literature. As it can be seen from Table 3. the Z coordinate where fracture occurred on the formed part (-Z frac) is about 20 mm. Using the part dimensions from Fig. 1(b) the final wall angle can be calculated, giving a value of 78.46°. This is higher than the published wall angle values of regular truncated conic shape which is used as reference geometry for evaluating the limit strains.

To summarize the result of the experiments an Interaction Plot of the factors for $-Z_{fraction}$ is given in Fig. 8.

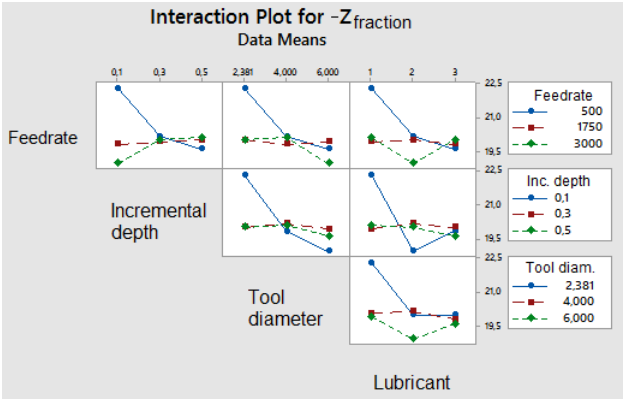

Fig. 8. Interaction of the factors for –Z fraction

Experimental results showed that tool diameter has the main influence on the forming depth in case of SPIF on AlMn1Mg1 sheets with 0.22 mm initial thickness, which reflects the importance of the t_0/R (initial sheet thickness to tool radius) ratio. The second factor in the line of the

influencing parameters is the lubrication (respect to Sommerfeld number) which is followed by the feedrate and the incremental depth.

Further analysis can be carried out by correlation matrix of parameters, which is displayed on Table 4. From that it follows, that highest correlation index is between tool diameter and forming depth, negative sign indicates that as lower the diameter as higher the depth. This fact supports the hypothesis that compressing stresses play a key role in the increased formability of SPIF, as smaller diameter induces compressive stresses more effectively in the surface of sheet.

Second highest indices can be regarded to feedrate and lubrication but the effect of △z incremental depth is less significant. This ranking is in good agreement with the conclusions derived from Fig. 8.

Table 4. Correlation matrix of parameters

	F	Δz	*d*	*Lubr.*	*-Z frac.*
F	1				
⊿z	0.130	1			
d	0.126	0.126	1		
Lubr.	-0.130	-0.130	-0.126	1	
-Z frac.	-0.574	-0.385	-0.661	0.564	1

As lubricant is not a quantified parameter, only tool diameter and feedrate have been analysed by multiple regression. Equation (3) shows the result of numerical calculation:

$$-Z_{frac.} = 22.8 - 0.42 \cdot d - 0.0005 \cdot F \qquad (3)$$

The coefficient of regression is 0.826, which is acceptable for further estimation of forming depth if the same sheet metal is used.

IV. CONCLUSIONS AND OUTLOOK

In this paper, the characterization of AlMn1Mg1 and Single Point Incremental Forming of the same material with 0.22 mm initial thickness have been conducted, applied a Design of Experiments using L9 orthogonal array of Taguchi.

The monitoring of servo motor currents allowed the estimation of the forming forces. All results regarding the estimation of fracture caused by necking are consonant with the results obtained in SPIF of thicker sheets.

Further investigations could be conducted in order to study the influence of lubrication.

V. ACKNOWLEDGMENTS

The research presented in this paper was carried out as part of the EFOP-3.6.2-16-2017-00016 project in the framework of the New Széchenyi Plan. The completion of this project is funded by the European Union and co-financed by the European Social Fund.
The support provided by T. Gyoger and Sz. Szalai in the experiments is also greatly acknowledged.

REFERENCES

[1] **Duflou, J.; Tunçkol, Y.; Szekeres, A.; Vanherck, P.**: Experimental study on force measurements for single point incremental forming, *Journal of Materials Processing Technology*, Vol. 189, Issues 1-3, 2007, pp. 65-72.

[2] **Bagudanch, I.; Centeno, G.; Vallellano, C.; Garcia-Romeu, M.L.**: Forming Force in Single Point Incremental Forming under Different Bending Conditions, *Procedia Engineering*, Vol. 63, 2013, pp. 354-360.

[3] **Thibaud, S.; Ben Hmida, R.; Richard, F.; Malécot, P.**: A fully parametric toolbox for the simulation of single point incremental sheet forming process: Numerical feasibility and experimental validation, *Simulation Modelling Practice and Theory*, Vol. 29, 2012, pp. 32-43.

[4] **Ben Hmida, R.; Thibaud, S.; Gilbin, A.; Richard, F.**: Influence of the initial grain size in single point incremental forming process for thin sheets metal and microparts: Experimental investigations, *Materials & Design*, Vol. 45, 2013, pp. 155-165.

[5] **Obikawa, T.; Satou, S.; Hakutani, T.**: Dieless incremental micro-forming of miniature shell objects of aluminum foils, *International Journal of Machine Tools and Manufacture*, Vol. 49, Issues 12–13, 2009, pp. 906-915.

[6] **Sekine, T.; Obikawa, T.**: "Micro Incremental Forming Characteristics of Stainless Foil", *Key Engineering Materials*, Vols. 447-448, 2010, pp. 346-350.

[7] **Gatea, S.; Ou, H.; McCartney, G.**: Review on the influence of process parameters in incremental sheet forming, *The International Journal of Advanced Manufacturing Technology*, 2016, pp. 1-21.

[8] **Hussain, G.; Gao, L.**: A novel method to test the thinning limit of sheet metal in negative incremental forming, *International Journal of Machine Tools and Manufacture*, 47, 2007, pp. 419-435.

[9] **Ambrogio, G.; Filice, L.; Micari, F.**: A force measuring based strategy for failure prevention in incremental forming, *Journal of materials processing technology*, Vol. 177., No. 1., 2006, pp. 413-416.

[10] **Rauch, M.; Hascoet, J. Y.; Hamann, J. C.; Plenel, Y.**: Tool path programming optimization for incremental sheet forming applications, *Computer-Aided Design*, Vol. 41., No. 12., 2009, pp. 877-885.

[11] **Paniti, I.; Viharos, Zs. J.**: Fracture diagnostics for Single Point Incremental Forming of thin Aluminum alloy foils, Proceeding of 15th IMEKO TC10 Workshop on Technical Diagnostics in Cyber-Physical Era, Budapest, Hungary, June 6-7, 2017, pp. 34-38.

[12] **Najm, S. M.; Paniti, I.**: Experimental Investigation on the Single Point Incremental Forming of AlMn1Mg1 Foils using Flat End Tools, IOP Conference Series: Materials Science and Engineering, Vol. 448, No. 1, 2018, November, p. 012032

[13] **Johnson, C. F.; Kiridena, V. S.; Ren, F.; Xia, Z. C.**, Ford Global Technologies LLC: System and method for incrementally forming a workpiece, 2012, U.S. Patent 8,322,176.

[14] **Meier, H.; Magnus, C.; Smukala, V.**: Impact of superimposed pressure on dieless incremental sheet metal forming with two moving tools. *Cirp Annals*, 60(1), 2011, pp. 327-330.

[15] **Paniti, I.; Somlo, J.**: Device for two sided incremental sheet forming, 2011, EU Patent EP2505279A1

[16] **Filice, L.; Fratini, L.; Micari, F.**: Analysis of Material Formability in Incremental Forming, *CIRP Annals*, Vol. 51/1/2002, pp. 199-202.

[17] **Micari, F.**: Single Point Incremental Forming: recent results, Seminar on Incremental Forming, 22 October 2004. Cambridge University. CD-ROM.

[18] **Kim, T.J.; Yang, D.Y.**: Improvement of formability for the incremental sheet metal forming process, *International Journal of Mechanical Sciences*, Vol. 42, 2001, pp. 1271-1286.

[19] **Jeswiet, J.; Hagan, E.; Szekeres, A.**: Forming Parameters for Incremental Forming of Aluminum Sheet Metal, *IMECHE part B, J. of Engineering Manufacture*, Vol. 216, 2002, pp. 1367-1371.

[20] https://www.gom.com/metrology-systems/argus.html, last visited: 26.06.2019.